Cardiovasc Intervent Radiol
https://doi.org/10.1007/s00270-019-02340-4

Combining Direct 3D Volume Rendering and Magnetic Particle Imaging to Advance Radiation-Free Real-Time 3D Guidance of Vascular Interventions

Dominik Weller[1] · Johannes M. Salamon[2] · Andreas Frölich[3] · Martin Möddel[4,5] · Tobias Knopp[4,5] · René Werner[1]

Received: 24 May 2019 / Revised: 31 August 2019 / Accepted: 6 September 2019

Abstract

Purpose Magnetic particle imaging (MPI) is a novel tomographic radiation-free imaging technique that combines high spatial resolution and real-time capabilities, making it a promising tool to guide vascular interventions. Immediate availability of 3D image data is a major advantage over the presently used digital subtraction angiography (DSA), but new methods for real-time image analysis and visualization are also required to take full advantage of the MPI properties. This laboratory study illustrates respective techniques by means of three different patient-specific 3D vascular flow models.

Material and Methods The selected models corresponded to typical anatomical intervention sites. Routine patient cases and image data were selected, relevant vascular territories segmented, 3D models generated and then 3D-printed. Printed models were used to perform case-specific MPI imaging. The resulting MPI images, direct volume rendering (DVR)-based fast 3D visualization options, and their suitability to advance vascular interventions were evaluated and compared to conventional DSA.

Results The experiments illustrated the feasibility and potential to enhance image interpretation during interventions by using MPI real-time volumetric imaging and problem-tailored DVR-based fast (approximately 30 frames/s) 3D visualization options. These options included automated viewpoint selection and cutaway views. The image enhancement potential is especially relevant for complex geometries (e.g., in the presence of superposed vessels).

Conclusion The unique features of the as-yet preclinical imaging modality MPI render it promising for guidance of vascular interventions. Advanced fast DVR could help to fulfill this promise by intuitive visualization of the 3D intervention scene in real time.

Keywords Magnetic particle imaging · Vascular imaging · 4D visualization · Real-time image processing

Dominik Weller and Johannes M. Salamon: Shared first authorship.

Electronic supplementary material The online version of this article (https://doi.org/10.1007/s00270-019-02340-4) contains supplementary material, which is available to authorized users.

✉ René Werner
r.werner@uke.de

[1] Department of Computational Neuroscience, University Medical Center Hamburg-Eppendorf, Martinistr. 52, 20246 Hamburg, Germany

[2] Department of Diagnostic and Interventional Radiology and Nuclear Medicine, University Medical Center Hamburg-Eppendorf, Martinistr. 52, 20246 Hamburg, Germany

[3] Department of Diagnostic and Interventional Neuroradiology, University Medical Center Hamburg-Eppendorf, Martinistr. 52, 20246 Hamburg, Germany

[4] Section for Biomedical Imaging, University Medical Center Hamburg-Eppendorf, Lottestr. 55, 22529 Hamburg, Germany

[5] Institute for Biomedical Imaging, Hamburg University of Technology, Schwarzenbergstr. 95C, 21073 Hamburg, Germany

Published online: 16 September 2019

Introduction

Magnetic particle imaging (MPI) is a radiation-free tomographic imaging technique that uses superparamagnetic iron oxide nanoparticles (SPIOs) as tracer [1]. By exploiting the magnetization behavior of SPIOs, magnetic fields can be utilized to reconstruct 3D MPI images of spatial tracer distributions at scan rates of up to 46 frames per second. Detection of the magnetic particles can be performed with good spatial resolution (<1 mm), high sensitivity and high signal-to-noise ratio [2]. Furthermore, in an early animal experiment, Weizenecker et al. [3] proved applicability of MPI in vivo using a clinically approved MRI contrast agent (Resovist/Ferucarbotran) as tracer substance.

Based on these unique properties, MPI has emerged as a promising tool in biomedical imaging. Its ability to quantitatively assess 3D tracer dynamics with high temporal resolution qualifies MPI as a favorable future modality for real-time vascular imaging. First steps toward clinical implementation in interventional medicine have been described in proof-of-principle studies that demonstrated feasibility of engineering a tracer-coated catheter suitable for use in vascular interventions [4] and differentiated tracer-coated devices and tracer-marked fluid in a vessel phantom [5]. The envisioned application in [5] was to simultaneously visualize and encode, for example, vascular tree/the blood pool and instruments during intervention using different colors to facilitate navigation and instrument localization; this is referred to as multi-color (multispectral) MPI. Moreover, the strong magnetic fields in MPI scanners could even be used to apply torques and forces on magnetic catheters [6].

However, the clinical gold standard for vascular imaging in interventional medicine is currently digital subtraction angiography (DSA) with time-controlled X-rays. The major disadvantages of this are well known: the risk of the ionizing radiation dose, and the difficult spatial interpretation of complex vascular geometries, due to insufficient depth information and superposed projections of different structures. Proposed approaches to enhance intra-procedural vascular visualization are fusion of fluoroscopic images with pre-procedurally acquired computed tomography angiography (CTA) or magnetic resonance angiography (MRA) datasets. The resulting 3D roadmapping has been shown to reduce the radiation dose, procedure length and volume of injected contrast agent for vascular interventions by reducing the need for repeated DSA runs [7–10]. However, 2D-to-3D image registration is susceptible to patient movements and overlay accuracy is limited by respiratory and cardiac motion as well as device-related vessel deformation.

In contrast, MPI is neither dependent on external image data nor dependent on application of error-prone co-registration. Using multi-color MPI, a dynamic 3D vessel roadmap and medical device positions can be simultaneously captured with high temporal resolution. As MPI is radiation-free, imaging can be performed continuously during intervention, ensuring gapless monitoring of tracer-coated devices and intervention success. This, in turn, offers ideal conditions for online as well as retrospective quality assurance of interventions.

However, MPI scanners are still in a preclinical state and application is limited to phantoms and small animals. With a focus on cardiovascular interventions, Herz et al. [11] recently pointed out that especially current MPI visualization latencies preclude clinical application. Yet, they also showed that the latencies can be sufficiently reduced to allow real-time visualization of at least 2D projections of vascular structures and instruments.

As such, to fully exploit the potential of interventional MPI, we consider it similarly essential to develop suitable visualization frameworks to provide precise but also intuitively interpretable representations of the complex spatio-temporal (i.e., 3D + time) MPI data that meet practical needs in endovascular real-time navigation. This laboratory study aims to illustrate opportunities opened up by combining MPI image information with advanced visualization options, in our case direct volume rendering (DVR). To demonstrate presumed benefits of MPI real-time 3D visualization, real-time MPI imaging of patient-specific vasculature models corresponding to typical anatomical intervention sites was performed. This enabled a realistic comparison with conventional imaging and image impression.

Materials and Methods

Selection of Use Cases and Patient Data

Three clinical use cases were defined with regard to clinical relevance and assumed added value through improved intra-procedural visualization of the associated vascular site. Corresponding patient cases were selected from a pool of anonymized CT and flat panel CT datasets.

The first case comprised a sacciform aneurysm located at the carotid siphon of the internal carotid artery (ICA), a typical site for endovascular coiling. The second case covered segments M1 and M2 of the middle cerebral artery (MCA), i.e., the most common site of occlusion in thrombotic cerebral ischemia [12] and a typical site for mechanical thrombectomy. The third case covered the hepatic vascular system, where a common intervention is transarterial chemoembolization to selectively occlude

Table 1 Overview of considered anatomic structures, original image dataset characteristics, typical interventions and associated intervention-related challenges for each structure

Model	Anatomic structure	Original imaging modality	Voxel resolution of original image data	Typical associated intervention	Assumed intervention-specific challenge
1	Internal carotid artery aneurysm (saccular shape)	FP-CT	$0.1 \times 0.1 \times 0.1$ mm^3	Endovascular coiling	Precise placement of coils
2	Middle cerebral artery (segment M1/M2)	FP-CT	$0.1 \times 0.1 \times 0.1$ mm^3	Mechanical thrombectomy	Fast and safe navigation to occlusion site
3	Proper hepatic artery	CE-CT	$0.87 \times 0.87 \times 1$ mm^3	Transarterial chemoembolization	Precise intra-operative catheter alignment along vessel course

FP-CT flat panel computed tomography, *CE-CT* contrast-enhanced computed tomography

pathologic tumor parent arteries [13]. For further details, see Table 1.

Workflow, Part I: From Clinical Image Data to Patient-Specific MPI Imaging

The study workflow is summarized in Fig. 1. To enable for patient-specific acquisition of MPI image data with currently available preclinical MPI scanners, a 3D-printed model of the relevant vascular territory was generated as the starting point (Fig. 1, panels A–C). This comprised semi-manual vessel segmentation using the original clinical image data (Table 1) and conversion of the segmentation data into triangulated surface models and standard tessellation language (STL) files, using the software 3D Slicer[1] [14]. Refinement and adjustments of the generated surface models (surface smoothing, attachment of tube connections and holding devices required for subsequent workflow steps) were performed using Blender.[2] 3D printing of the resulting vasculature models was completed by a stereolithography laser printer (Form 2, Formlabs, Somerville, USA; printing resolution: 0.05 mm; materials: Formlabs Form 2 Clear Resin).

As denoted in Figs. 1D–E, the printed 3D models were connected to a flow system. This system consisted of a water pump (DC Runner 5.1, Aqua Medic, Bissendorf, Germany), an aqua tank and an angiographic catheter used for tracer injection (Radifocus Optitorque, Terumo, Somerset, USA). The models were then positioned in the MPI scanner (Bruker Biospin GmbH, Ettlingen, Germany). Subsequently, a 1.5 ml tracer bolus of Resovist (108 mg/ml) was injected and MPI data acquisition started. Applied flow rates during scanning ranged between 160 and 200 ml/min, approximately resembling physiological blood flow rates [15, 16]. Data were acquired using a selection gradient field of 1.5 T/m and a drive field of 14 mT. Measurements were repeated multiple times to ensure reproducibility.

Workflow, Part II: MPI Image Reconstruction and 3D DVR-Based Visualization

Image reconstruction (Fig. 1F) was based on a system function approach [17] and using an online MPI reconstruction framework [18]. Resulting voxel resolution of the individual frames was $2 \times 2 \times 1$ mm^3 (field-of-view: $50 \times 50 \times 25$ mm^3); imaging frequency was 46 frames/s.

To overcome limitations of typical slice-wise representation of the image information and/or multiplanar reconstruction, we implemented direct volume rendering (DVR)-based visualization variants using the visualization toolkit VTK.[3] The principle of volume rendering is summarized in Fig. 2. In addition, standard DVR-based MPI image visualization was augmented by problem-tailored online image analysis and visualization options:

Dynamic Build-Up of a 3D Roadmap

To enhance image series interpretability and to form the basis of the subsequent analysis steps, a 3D roadmap of the vascular geometry was built up by piecewise image accumulation of the bolus motion during its first throughflow cycle. A vessel centerline was extracted from the final 3D roadmap using the VMTK library.[4]

Auto-Focus on Target Area Structures and Instrument Position

Superposed vessels along the view rays impede scene interpretability due to resulting occlusions. Based on the

[1] www.slicer.org

[2] www.blender.org

[3] www.vtk.org

[4] www.vmtk.org

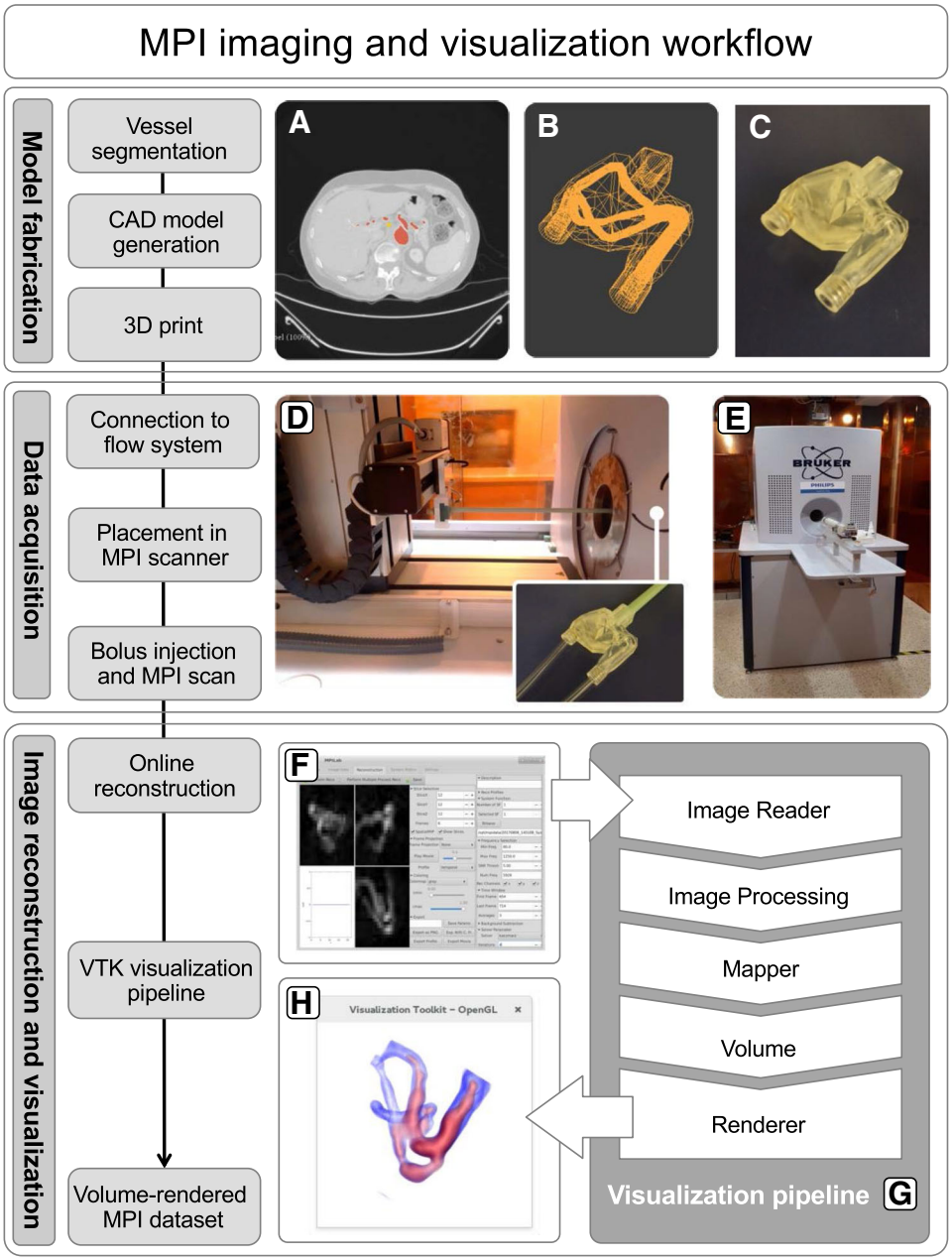

Fig. 1 Study workflow. Segmented vessels for each use case (**A**) were transformed into polygon meshes of the vessel geometry and a corresponding 3D model (**B**). The vascular model was 3D-printed (**C**) with transparent resin, allowing visual control of the vessel geometry. The printed models were connected to a flow system and placed in the MPI scanner (**D**–**E**). Image reconstruction was performed online (**F**), and the reconstructed image datasets processed (pipeline shown in **G**) and visualized (**H**)

centerline representation of the vascular geometry and known instrument/target position, a cutaway view was implemented that ignores ray tracing contributions by vessels and voxel that are too distant from the target structure centerline(s).

Automated Viewpoint Optimization

To further facilitate instrument navigation, an automated viewpoint and virtual camera position optimization were implemented. This maximized visibility of the geometry centerline segments connecting instrument tip and target position, i.e., the remaining path of the instrument during intervention.

Comparison of MPI DVR and Conventional MIP Visualization

To qualitatively compare MPI DVR data visualization with conventional image representation, maximum-intensity projections (MIP) were derived from the clinical use case image datasets. The focus of the evaluation was the visibility of relevant use case-specific anatomical details.

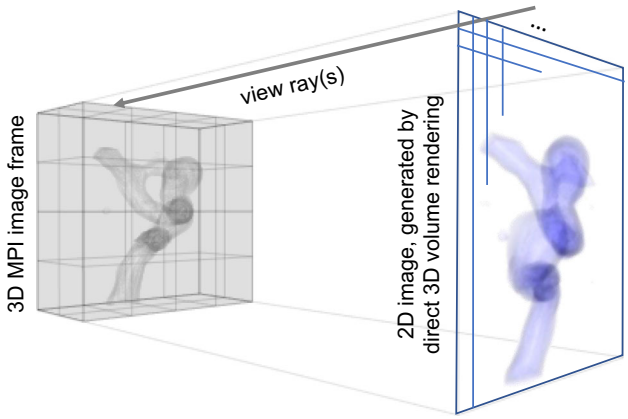

Fig. 2 Principle of direct volume rendering (DVR), here: volume ray casting. Originating from a virtual camera in front of the desired 2D output image, view rays are sent through the image pixels into the scene to be visualized—in this case the reconstructed 3D MPI image volume. The ray is sampled throughout the volume, and the image intensity values at the sampling points are converted to RGBA (red, green, blue, alpha; common color model) values via a transfer function. The accumulated RGBA values determine the final 2D output image. The reconstructed 3D image volume can be virtually rotated or moved before sending the rays to traverse the scene. This enables visualization of the structures of interest (vascular geometries in this image) from different perspectives and viewpoints

Results

Figures 3, 4, 5 and 6 illustrate MPI DVR visualization for the considered use cases; corresponding videos representing the flow dynamics are provided as supplemental materials. Subsequent observations are based on visual inspection and image perception by the authors and are therefore subjective. To allow the reader to get a more detailed idea, the source code and the MPI data are available at https://github.com/IPMI-ICNS-UKE/MPI-DVR. Frame rates of the DVR visualization depend on various parameters such as the size of the display window or the MPI image size. Mean rates of the provided source code (not run-time optimized) were in the order of 30 frames/s on a standard PC (Intel Core i5-7300HQ CPU 2.5 GHz, 8 GB RAM, GeForce GTX 1050 Ti), fulfilling real-time requirements.

Visualization of ICA Aneurysm

Figure 3 illustrates that time-resolved 3D bolus visualization of the dynamic MPI data allowed for intuitive qualitative assessment of the flow distribution within the aneurysm and the parent artery. In particular, the morphological shape of the aneurysm and the demarcation between parent artery and aneurysm neck, which plays an important role in the clinical context, were clearly visible using volume-rendered visualization. This is in contrast to standard anterior–posterior 2D MIP data visualization.

MCA Visualization

Similar to the first use case, MPI DVR permitted rapid visual assessment of bolus dynamics and flow distribution. The 3D roadmap enabled accurate characterization of the vessel geometry (Fig. 4). Yet, the applied default DVR viewpoint and visualization did not allow the observer to estimate the spatial distance between the virtual guide wire tip and target position (Fig. 6A; no catheter movement simulated). Here, automated viewpoint optimization proved its potential by adjustment of the DVR virtual camera position in order to maximize the visible centerline length between the guide wire tip and target location for different viewing angles (Fig. 6B). After optimization, the vessel segment of interest was accurately displayed.

Hepatic Artery Visualization

DVR visualization of the vascular branches of the hepatic artery revealed their spatial course (Fig. 5). However, intuitive interpretability of the complex vascular geometry was affected by partial volume artifacts and superposed vessels. Figure 5I, J illustrates respective benefit when applying the developed centerline-based cutaway view. This results in a visualization that is restricted to the relevant structures: a virtual guide wire tip and the targeted vessel area. In addition, Fig. 6E–I again illustrates the advantages of automated viewpoint. Note that, as with the other use cases, the corresponding tools only become effective by combining real-time volumetric imaging, image visualization and image analysis.

Discussion

In the current laboratory study, DVR was introduced as a 3D visualization option capable of rendering temporal volumetric MPI image sequences in real time.

The suitability of combining MPI imaging and DVR-based visualization to enhance intuitive image and scene interpretation during vascular intervention was illustrated by three selected real-patient vascular geometries. Also implemented were problem-tailored image analysis and visualization options (centerline-based 3D roadmap build-up; cutaway views; automated viewpoint and camera positioning optimization) to augment standard DVR-based image visualization. These options countered the existing challenges in endovascular interventions: estimation of spatial distances (which appear distorted when projected

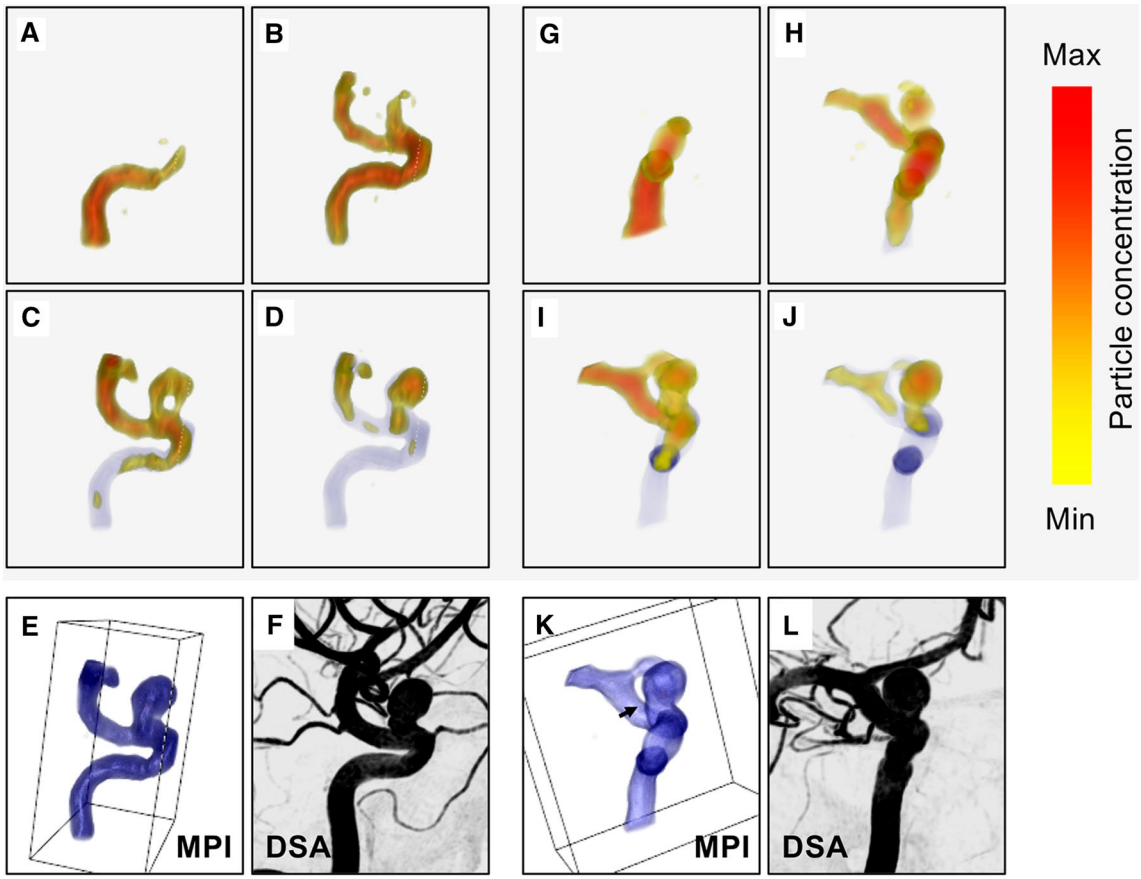

Fig. 3 DVR-based visualization of MPI data of a sacciform aneurysm located in the internal carotid artery. Images with a gray background show the temporal dynamics of the bolus from the lateral (**A**–**D**) and anterior–posterior (**G**–**J**) viewpoints. For MPI, voxel image intensity corresponds to local particle concentration (color coding: red = high concentration; yellow = low concentration). Panels **E**–**F** and **K**–**L** depict the generated 3D MPI roadmap and reconstructed MIP data (similar to a clinical DSA image) from the same perspective. In contrast to the 2D projection data, the 3D visualization allows for identification and assessment of morphological details like the outgoing aneurysm neck (arrow)

onto two dimensions) and navigation at vessel bifurcations (especially in the presence of superposed vessels).

Major limitations of our study are directly related to its character as a proof-of-concept study. The three patient cases were selected to represent typical intervention sites; however, no real-time intervention was performed and the selected scenarios do not allow demonstrating the efficacy of DVR-based visualization during cardiovascular interventions in general.

Moreover, the study was aimed only at qualitative illustration of feasibility and suitability, with the subjective assessment of the images performed by the authors. A comprehensive and quantitative evaluation of the visualization options in a scenario closer to the clinical reality is regarded as the next step. In order to further improve the developed tools, this would comprise the use of clinical DSA data (instead of retrospectively computed MIP images) and detailed analysis of related clinical working procedures (e.g., how often are C-arm positions changed to improve sight of the target area? What are relevant landmarks that the physician focuses on?). Nevertheless, to allow the reader to form their own opinion, the source code and MPI data of our study are available as open source.

DVR was already reported to be superior to surface-based rendering techniques for localization of complex vessel branches compared to standard MIP visualization over a decade ago. However, it has also been described as challenging in terms of display parameter selection and transfer function selection [19]. As such, MPI as a background-free imaging modality is ideally suited for automated and standardized transfer function design: There is no image information to be displayed other than the signal-generating SPIO tracer. Therefore, although based on selected cases, our observations are in line with prior findings in the context of 3D medical image visualization, and we assume the illustrated advantages to be transferable to different endovascular procedures and situations.

From a technical perspective, our study demonstrates that DVR-based 3D visualization of MPI image data fulfills real-time capabilities. However, in terms of an intended

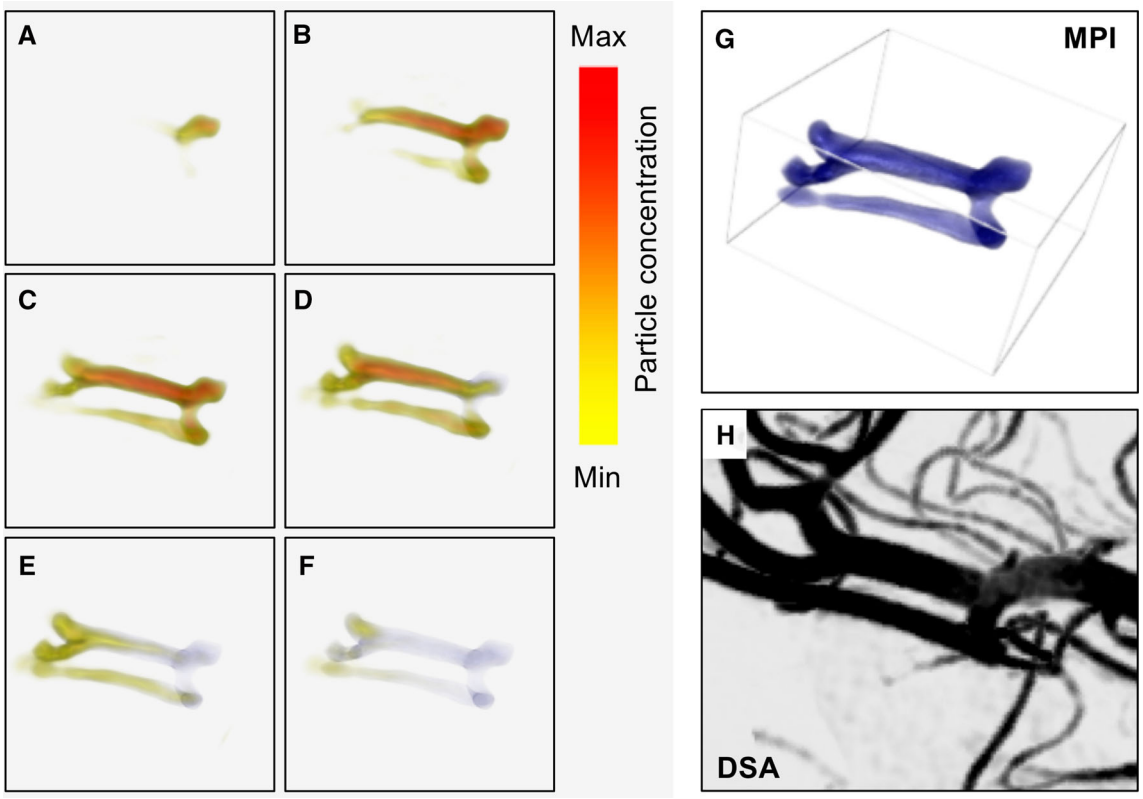

Fig. 4 DVR-based visualization of middle cerebral artery (MCA), successor branches and respective flow dynamics. Panels **A**–**F** depict the bolus dynamics using intensity-based color coding (as per Fig. 3). Panel **G** represents the reconstructed static 3D roadmap within the corresponding MPI field-of-view. Panel **H** depicts a DSA-like MIP reconstruction derived from the original flat panel CT dataset of the patient

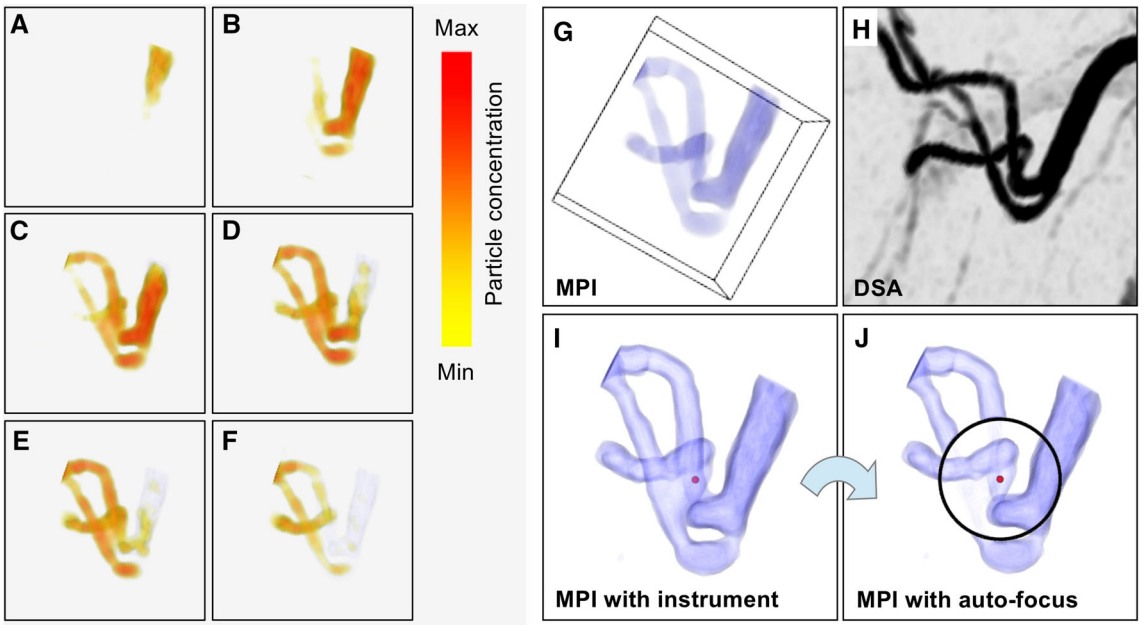

Fig. 5 DVR-based visualization of hepatic artery, subsequent branches and flow information. Panels **A**–**F** represent the dynamic color-coded visualization of the bolus inflow. The resulting 3D roadmap within the MPI field-of-view (**G**) is compared to the reconstructed DSA-like 2D MIP reconstruction (**H**). Visualization of a virtual catheter tip (red sphere) positioned in the posterior vessel branch was enhanced by application of a cutaway view (**I**, **J**). The roadmap visualization contained superimposed vessels and overlapping vessel boundaries (arrow); such geometry ambiguities can be resolved by analysis of the dynamics of the bolus front

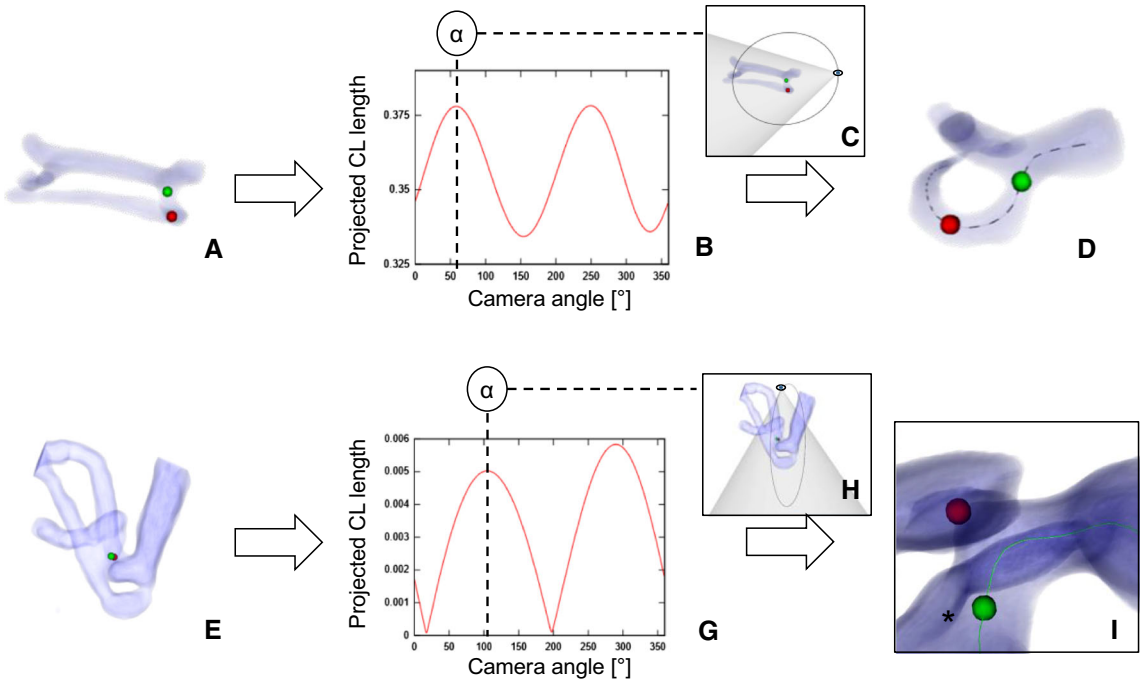

Fig. 6 Examples of automatic viewpoint selection. The starting situations, viewed from a default viewing angle and camera position, are shown in panels **A** and **E**. To optimize visibility of the vessel segment(s) between two target points (red and green spheres), the virtual camera is rotated along the circular trajectories depicted in **C** and **H**. By analysis of the length of the projected center line(s) between the target points, optimal viewing angles (α) are determined (**B**, **G**), resulting in the views shown in **D** and **I**. Due to the symmetrical nature of the problem in **A**–**D**, two maxima exist in **B**; in such a case, a view from a cranial perspective was preferred. In **D**, a line consisting of sections of equal size was used to further accentuate the extension of the vascular geometry. In **I**, the centerline visualization was helpful to keep track of the original course of the targeted artery despite existence of overlapping vessel boundaries

future clinical application, the entire imaging pipeline has to work in real time. In the present study, we applied an online reconstruction with a latency of about 2 s [18], which would preclude clinical application. Nevertheless, reconstruction approaches with significantly reduced latencies are already under development [11].

Ongoing MPI developments will further strengthen suitability of MPI as a future interventional imaging modality. These include: imaging of long-lasting blood pool tracers [20], the identification and optimization of alternative tracer materials that promise higher sensitivity and spatial resolution than Resovist [21], trends toward multi-patch reconstruction for effective imaging of a larger field-of-view to overcome further limitations of current preclinical MPI systems [22], and optimized image processing enabling, e.g., more precise tracer-marked device tracking [23].

Conclusion

The capability of MPI to provide volumetric images in real time without the use of ionizing radiation renders it promising for guidance of vascular interventions. Advanced fast 3D visualization options—such as direct volume rendering, detailed in the present study—will help to fulfill this promise by immediate and intuitively interpretable visualization of the 3D intervention scene.

Acknowledgements We acknowledge funding by the German Research Foundation (Grant Number KN 1108/2-1) and the Federal Ministry of Education and Research (Grant Numbers 05M16GKA, 13XP5060B).

Compliance with Ethical Standards

Conflict of interest René Werner receives a research grant from Siemens Healthcare GmbH (not related to present study). Tobias Knopp receives a research grant from Philips GmbH Innovative Technologies (not related to the present study).

References

1. Gleich B, Weizenecker J. Tomographic imaging using the nonlinear response of magnetic particles. Nature. 2005;435:1214–7.
2. Borgert J, Schmidt JD, Schmale I, Rahmer J, Bontus C, Gleich B, et al. Fundamentals and applications of magnetic particle imaging. J Cardiovasc Comput Tomogr. 2012;6:149–53.
3. Weizenecker J, Gleich B, Rahmer J, Dahnke H, Borgert J. Three-dimensional real-time in vivo magnetic particle imaging. Phys Med Biol. 2009;54:L1–10.
4. Haegele J, Panagiotopoulos N, Cremers S, Rahmer J, Franke J, Duschka RL, et al. Magnetic particle imaging: a Resovist based

marking technology for guide wires and catheters for vascular interventions. IEEE Trans Med Imaging. 2016;35(10):2312–8.
5. Rahmer J, Halkola A, Gleich B, Schmale I, Borgert J. First experimental evidence of the feasibility of multi-color magnetic particle imaging. Phys Med Biol. 2015;60:1775–91.
6. Rahmer J, Wirtz D, Bontus C, Borgert J, Gleich B. Interactive magnetic catheter steering with 3-D real-time feedback using multi-color magnetic particle imaging. IEEE Trans Med Imaging. 2017;36(7):1449–56.
7. Stangenberg L, Shuja F, Carelsen B, Elenbaas T, Wyers MC, Schermerhorn ML. A novel tool for three-dimensional roadmapping reduces radiation exposure and contrast agent dose in complex endovascular interventions. J Vasc Surg. 2015;62(2):448–55.
8. Bargellini I, Turini F, Bozzi E. Image fusion of preprocedural CTA with real-time fluoroscopy to guide proper hepatic artery catheterization during transarterial chemoembolization of hepatocellular carcinoma: a feasibility study. Cardiovasc Interv Radiol. 2013;36:526–30.
9. Van den Berg JC. Update on new tools for three-dimensional navigation in endovascular procedures. Aorta (Stamford). 2014;2(6):279–85.
10. Zhang Q, Sun Q, Zhang Y, Zhanf H, Shan T, Han J, et al. Three-dimensional image fusion of CTA and angiography for real-time guidance during neurointerventional procedures. J Neurointerv Surg. 2017;9:302–6.
11. Herz S, Vogel P, Dietrich P, Kampf T, Rückert MA, Kickuth R, et al. Magnetic particle imaging guided real-time percutaneous transluminal angioplasty in a phantom model. Cardiovasc Interv Radiol. 2018;41:1100–5.
12. Hossmann KA, Heiss WD. Ch.1. In: Brainin M, Heiss WD, editors. Textbook of stroke medicine. Cambridge University Press: Cambridge; 2009. p. 1–27.
13. Clark TW. Complications of hepatic chemoembolization. Semin Interv Radiol. 2006;23:119–25.
14. Fedorov A, Beichel R, Kalpathy-Cramer J, Finet J, Fillion-Robin JC, Pujol S, et al. 3D Slicer as an image computing platform for the quantitative imaging network. Magn Reson Imaging. 2012;30:1323–41.
15. Zarrinkoob L, Ambarki K, Wåhlin A, Birgander R, Eklund A, Malm J. Blood flow distribution in cerebral arteries. J Cereb Blood Flow Metab. 2015;35(4):648–54.
16. Carlisle KM, Halliwell M, Read AE, Wells PN. Estimation of total hepatic blood flow by duplex ultrasound. Gut. 1992;33(1):92–7.
17. Weber A, Werner F, Weizenecker J, Buzug TM, Knopp T. Artifact free reconstruction with the system matrix approach by overscanning the field-free-point trajectory in magnetic particle imaging. Phys Med Biol. 2016;61:475–87.
18. Knopp T, Hofmann M. Online reconstruction of 3D magnetic particle imaging data. Phys Med Biol. 2016;61(11):N257–67.
19. Fishman EK, Ney DR, Heath DG, Corl FM, Horton KM, Johnson PT. Volume rendering versus maximum intensity projection in CT angiography: what works best, when, and why. Radiographics. 2006;26(3):905–22.
20. Rahmer J, Antonelli A, Sfara C, Tiemann B, Gleich B, Magnani M, et al. Nanoparticle encapsulation in red blood cells enables blood-pool magnetic particle imaging hours after injection. Phys Med Biol. 2013;58:3965–77.
21. Kaul M, Mummert T, Jung C, Salamon J, Khandhar A, Ferguson M, et al. In vitro and in vivo comparison of a tailored magnetic particle imaging blood pool tracer with Resovist. Phys Med Biol. 2017;62:3454–69.
22. Szwargulski P, Möddel M, Gdaniec N, Knopp T. Efficient joint image reconstruction of multi-patch data reusing a single system matrix in magnetic particle imaging. IEEE Trans Med Imaging. 2019;38:932–44.
23. Griese F, Knopp T, Werner R, Schlaefer A, Möddel M. Sub-millimeter-accurate marker localization within low gradient magnetic particle imaging tomograms. Int J Mag Part Imaging. 2017;3(1):1703011.